Image data assimilation with filtering methods

Anne Cuzol, Jean-Louis Marchand, Etienne Mémin

Image data assimilation with filtering methods

Anne Cuzol [1], Jean-Louis Marchand [2], Etienne Mémin [3]

[1] Univ. Bretagne-Sud, UMR 6205, LMBA, F-56000 Vannes
[2] ENS Rennes, Campus Universitaire de Kerlann, 35000 Bruz
[3] INRIA Rennes-Bretagne Atlantique

Abstract

In this paper we describe several techniques formulated within the stochastic filtering framework for image data assimilation issues. We advocate here the use of hybrid methods between ensemble Kalman methods and particle filters. The former family, despite being theoretically deficient in the sense that it does not in general converge towards the sought-after filtering moments, has demonstrated to be very efficient in practice for high dimensional space filtering issues. At the opposite, the latter are theoretically well posed but face strong practical difficulties in high dimensional spaces. We list here briefly the principal ideas of the underlying hybrid filters, their qualities and their drawbacks. Some comparison results between those different techniques are provided for the filtering of a 2D turbulent flow.

1 Introduction

Data assimilation techniques aim at coupling a system state dynamics with partially observed measurements of this system. Such a procedure is essential for instance in forecasting applications to estimate from observed data a good initial state of the system's variables or to calibrate dynamical parameters. A recent new challenge is emerging in geophysical flow analysis with the availability of high resolution satellite image data [Beyou et al., 2013, Corpetti et al., 2009, Titaud et al., 2010]. The assimilation of such data into oceanic or atmospheric numerical models is unfortunately not as easy as it may appear at a very first glance. As a matter of fact, it is immediate to feel like incorporating in weather

numerical models complex non linear phenomena such as fronts, or tornados that are evidently observed in image data sequences, and which are, in the same time, difficult to generate spontaneously from models. The essential difficulty of image assimilation ensues principally from the fact that the observed luminance does not belong to the system state space. In general, there is indeed a complex relation between the luminance function and the flow state variables. This complex relation leads to difficult inverse problems to recover for instance velocity, temperature or pressure variables from a set of images. The other source of concern lies in the fact that images and models do not live at the same scales. As a matter of fact, the spatial resolution of images are nowadays defined on finer spatial grids than models. This still increasing scale difference, due to satellite sensors technological progress, induces a scale relation which complicates further the connection between the state variables and the observations. Besides, large scale models are only imperfectly known. Small scale forcing and geophysical turbulence models for instance must be set up. The alternative, to specify such imperfect large scale evolution models consists in the establishment of stochastic dynamics where the uncertainty is formalized through stochastic processes [Franzke and Majda, 2005, Majda et al., 1999, Mémin, 2013]. In this latter case, it is important to point out that we are in a situation where the model random uncertainty is usually much more pregnant than the measurement noise defined at a higher resolution. This extreme case of quasi negligible data noise leads in particular to a badly conditioned situation for data assimilation procedures.

The coupling of a a partially known stochastic dynamics and noisy observations can be expressed through a nonlinear stochastic filtering problem. In the case of image data this filtering problem involves an evolution law of a state variable $\mathbf{x} \in \mathbb{R}^d$ of the form

$$\mathrm{d}\mathbf{x}_t = \mathbf{M}(\mathbf{x}_t)\mathrm{d}t + \sigma(\mathbf{x}_t)\mathrm{d}\mathbf{B}_t, \tag{1}$$

accompanied by partial observations of the system through measurements $\mathbf{y} \in \mathbb{R}^p$

$$\mathbf{y}_{t_k} = \mathbf{H}(\mathbf{x}_{t_k}) + \gamma_{t_k}. \tag{2}$$

In this system, both the dynamical operator, $\mathbf{M}$, and the observation operator, $\mathbf{H}$, between the measurement space and the state space are, in the general case, nonlinear. The observation equation (2) is in addition discrete in time due to a possibly long time interval between two consecutive measurements. The dynamics is at the opposite continuous with a discrete scheme associated to a much shorter time step. Concerning this stochastic dynamics, we will assume the dynamical noise is a Wiener process where the diffusion tensor, σ, may eventually depend

on the stochastic process, which gives rise in that case to multiplicative noises. As for the observation noise, γ_{t_k}, it can be non-Gaussian, but it is, nevertheless, conditionally independent of the state variable.

Beyond the main difficulty faced here, which concerns essentially the high dimensionality of the system ($\sim 10^6 - 10^9$), let us note the modeling of a proper stochastic representation of a state variable dynamics is in general not a straightforward stage. Several different directions can be followed depending on the application targeted. This goes from the definition of stochastic representations of deterministic pdes to the constitution of "inexact" evolution laws incorporating errors or uncertainties. In this article we will not elaborate on such issues and consider that the dynamics has been well defined and follows general form (1).

In the following we will present different solutions devised so far for the filtering of image data. Those techniques have all in common to be based on Monte Carlo principles. The first family of methods ensues from a Monte Carlo implementation of the Kalman filtering equations and incorporates efficient procedures to cope with matrix-vector products in high dimension. The second one concerns the so-called particle filters. It corresponds to a set of techniques that approximate the filtering distribution through a linear combination of Dirac masses centered on samples referred to as particles. In the following section we briefly describe those two types of methods. Advantages and deficiencies of both approaches are listed and we then describe, in a subsequent section, several hybrid techniques that aim at combining both families in order to keep the best of their properties. Some comparative results are provided in the last sections.

2 Assimilation with filtering methods

The first family of filtering methods is intensively used in geophysics. It relies on a Gaussian assumption and extends the Kalman update mechanisms through a Monte Carlo implementation.

2.1 Ensemble Kalman filter

The well-known Kalman filter [Kalman, 1960] allows to solve the filtering problem for linear Gaussian state-space models. At each time step, the Gaussian filtering distribution is characterised by its mean and covariance, which are recursively updated through the prediction and correction steps. In order to tackle the filtering problem for non linear and high-dimensional systems, Ensemble Kalman filters

have been developed [Evensen, 1994, Houtekamer and Mitchell, 1998, Bishop et al., 2001, Evensen, 2003, Ott et al., 2004]. These methods consist in a Monte Carlo approximation of the filtering distribution with particles that follow the prediction and correction steps of Kalman equations.

At time t_k, an approximation of the filtering distribution is given by :

$$\hat{p}(\mathbf{x}_{t_k}|\mathbf{y}_{t_1:t_k}) = \sum_{i=1}^{N} \delta_{\mathbf{x}_{t_k}^{(i)}}(\mathbf{x}_{t_k}), \tag{3}$$

where $\mathbf{x}_{t_k}^{(i)} \quad i = 1, \ldots, N$ are the particles (also called "ensemble members"). The prediction step consists in propagating the ensemble of particles $\mathbf{x}_{t_{k-1}}^{a,(i)}$ through the non-linear dynamics (including the model noise simulation) in order to obtain the predicted particles, or forecast ensemble $\{\mathbf{x}_{t_k}^{f,(i)}, i = 1, \ldots, N\}$. The empirical ensemble covariance matrix $\mathbf{P}_{t_k}^{f_e}$ is then deduced from the following expression:

$$\mathbf{P}_{t_k}^{f_e} = \frac{1}{N-1} \sum_{i=1}^{N} \left(\mathbf{x}_{t_k}^{f,(i)} - \overline{\mathbf{x}}_{t_k}^{f}\right) \left(\mathbf{x}_{t_k}^{f,(i)} - \overline{\mathbf{x}}_{t_k}^{f}\right)^T, \tag{4}$$

where the empirical mean of the forecast ensemble is defined by $\overline{\mathbf{x}}_{t_k}^{f} = \frac{1}{N} \sum_{i=1}^{N} \mathbf{x}_{t_k}^{f,(i)}$. The Kalman correction equation is then computed from this covariance matrix.

Since the Ensemble Kalman filter is based on a Gaussian assumption, it is known ([Le Gland et al., 2011]) that this filter does not converge towards the true filtering distribution for non linear systems. However, despite this theoretical drawback, this filter has been applied successfully to high-dimensional systems.

2.2 Particle filters

Particle filters [Gordon et al., 1993, Doucet et al., 2000, Del Moral, 2004] are able to solve exactly the filtering equations, up to the Monte Carlo approximation. In this class of methods, the filtering distribution is approximated by a weighted sum of particles :

$$\hat{p}(\mathbf{x}_{t_k}|\mathbf{y}_{t_1:t_k}) = \sum_{i=1}^{N} w_{t_k}^{(i)} \delta_{\mathbf{x}_{t_k}^{(i)}}(\mathbf{x}_{t_k}). \tag{5}$$

The particle filter is a sequential importance sampling technique: At each time step, particles $\{\mathbf{x}_{t_k}^{(i)}, i = 1, \ldots, N\}$ are first sampled from an importance distribution $\pi(\mathbf{x}_{t_k}|\mathbf{x}_{t_0:t_{k-1}}, \mathbf{y}_{t_1:t_k})$ (this corresponds to the prediction step). Then a new

weight $w_{t_k}^{(i)}$ is computed for each particle (correction step) using the following correction formulae :

$$w_{t_k}^{(i)} \propto w_{t_{k-1}}^{(i)} \frac{p(\mathbf{y}_{t_k}|\mathbf{x}_{t_k}^{(i)})p(\mathbf{x}_{t_k}^{(i)}|\mathbf{x}_{t_{k-1}}^{(i)})}{\pi(\mathbf{x}_{t_k}^{(i)}|\mathbf{x}_{t_0:t_{k-1}}^{(i)}, \mathbf{y}_{t_1:t_k})}.$$

The standard choice when applying the particle filter is to fix the proposal distribution to be the transition law $p(\mathbf{x}_{t_k}|\mathbf{x}_{t_{k-1}})$. In that case, it is easy to sample from the proposal (this requires only to sample from the dynamical model). However, this choice has the major drawback of sampling the particles without taking into account the observation $\mathbf{y}_{t_k}$. For high-dimensional systems, it has been proved that this standard particle filter can not be efficient in a general case [Snyder et al., 2008].

Different strategies can be however adopted in order to make the particle filter more efficient for high-dimensional models. First, one can define a precise dynamical model from the observations, aiming at reducing the dimension of the search space. This approach has been used in [Avenel et al., 2013] for the tracking of closed curves in images sequences. The dynamical model of the curve is constructed from the image data, and the dynamic uncertainty is reduced to a small-dimension noise (corresponding to normal and tangential perturbations of the curve). A low order dynamical representation based on radial basis functions has been used also successfully to track vorticity fields from images [Cuzol et al., 2007, Cuzol and Memin, 2009]. In both cases, which are associated to random field of low dimension, it has been shown that the simplest version of the particle filter can be successfully used.

Another way to cope with the curse of dimensionality associated to the usual blind sampling strategy of the bootstrap filter ($\pi(\mathbf{x}_{t_k}|\mathbf{x}_{t_0:t_{k-1}}, \mathbf{y}_{t_1:t_k}) \sim p(\mathbf{x}_{t_k}|\mathbf{x}_{t_{k-1}})$) consists in constructing importance distributions that integrate observations. This approach is presented briefly in the next section.

2.3 Hybrid filtering method

2.3.1 Idea

The importance distribution of the particle filter can be constructed in such a way that it integrates the observation $\mathbf{y}_{t_k}$ at each time step. In particular, one can use the Ensemble Kalman filter described in Section 2.1. This approach, called "Weighted Ensemble Kalman filter", has been proposed in [Papadakis et al., 2010]. It is close

to the technique proposed in [Van Leeuwen, 2010]. The importance distribution is taken as a Gaussian approximation of $p(\mathbf{x}_{t_k}|\mathbf{x}_{t_{k-1}}, \mathbf{y}_{t_k})$, obtained as output of the Ensemble Kalman filter. Each particle is then weighted. The Weighted ensemble Kalman filter (WEnKF) procedure can be simply summarized by Algorithm 1.

Algorithm 1 The WEnKF algorithm

For each $t_k = t_1, t_2, \ldots$:

- Start from particles set $\{\mathbf{x}_{t_{k-1}}^{(i)}, i = 1, \ldots, N\}$ and observation $\mathbf{y}_{t_k}$
- Obtain particles set $\{\mathbf{x}_{t_k}^{(i)}, i = 1, \ldots, N\}$ from:
  - **EnKF step:** Get $\mathbf{x}_{t_k}^{(i)}$, $i = 1, \ldots, N$, from the assimilation of $\mathbf{y}_{t_k}$ with an EnKF procedure;
  - **Computation of weights:** $w_{t_k}^{(i)} \propto w_{t_{k-1}}^{(i)} \frac{p(\mathbf{y}_{t_k}|\mathbf{x}_{t_k}^{(i)}) p(\mathbf{x}_{t_k}^{(i)}|\mathbf{x}_{t_{k-1}}^{(i)})}{p(\mathbf{x}_{t_k}^{(i)}|\mathbf{x}_{t_{k-1}}^{(i)}, \mathbf{y}_{t_k}^{(i)})}$;
  - **Resampling:** For $j = 1, \ldots, N$, sample with replacement index $I(j)$ from discrete probability $\{w_{t_k}^{(i)}, i = 1, \ldots, N\}$ over $\{1, \ldots, N\}$ and set $\mathbf{x}_{t_k}^{(j)} = \mathbf{x}_{t_k}^{I(j)}$. Set $w_{t_k}^{(i)} = \frac{1}{N} \quad \forall i = 1, \ldots, N$.

This filter combines the good properties of the ensemble Kalman mechanics with the correction scheme of the particle filter. Conceptually, this filter is more adapted to a non Gaussian distribution of the ensemble members, which is a situation that may arise at very short time horizon with nonlinear stochastic dynamics. The approach has been extended in [Beyou et al., 2013] for the assimilation of image observations, using a specific square-root filter (the Ensemble Transform Kalman filter) for the proposal step. We present below some results obtained with this method.

2.3.2 Application

State-space model In [Beyou et al., 2013], the state-space model is described by a stochastic version of the 2D Navier-Stokes equation for incompressible flows :

$$\mathrm{d}\boldsymbol{\xi}_t = -\nabla\boldsymbol{\xi}_t \cdot \mathbf{w}\mathrm{d}t + \nu\Delta\boldsymbol{\xi}_t\mathrm{d}t + \eta\mathrm{d}\mathbf{B}_t \tag{6}$$

where ν is the viscosity coefficient (inverse of the flow Reynolds number) and $\mathrm{d}\mathbf{B}_t$ is a random forcing term. The variable $\xi(\mathbf{x})$ denote the scalar vorticity at point $\mathbf{x} = (x, y)^T$, associated to the 2D velocity $w(\mathbf{x}) = (w_x(\mathbf{x}), w_y(\mathbf{x}))^T$ through $\xi(\mathbf{x}) = \frac{\partial w_y}{\partial x} - \frac{\partial w_x}{\partial y}$. The vector $\boldsymbol{\xi} \in \mathbb{R}^{|\Omega|}$ describes the vorticity over a spatial domain Ω of size $|\Omega|$, and $\mathbf{w} \in \mathbb{R}^{2|\Omega|}$ is the associated velocity field over the same domain. In practice, the model perturbations are simulations of random fields, correlated in space through a given covariance model. The value of η and the parameters of the covariance model have to be chosen.

This dynamical model is associated to a non linear observation equation based on the luminance (color intensity of images) conservation along fluid trajectories, up to a Gaussian noise :

$$I_{t_k}(\mathbf{x}) = I_{t_{k+1}}(\mathbf{x} + \mathbf{d}(\mathbf{x})) + \gamma_{t_k}(\mathbf{x}) \quad \forall \mathbf{x} \in \Omega_I, \tag{7}$$

where I is the luminance function, Ω_I is the spatial image domain, and $\mathbf{d}(\mathbf{x}) = \int_{t_k}^{t_{k+1}-\delta t} \mathbf{w}_t(\mathbf{x}_t)\mathrm{d}t$ denotes the displacement between time t_k and time t_{k+1}, with $\mathbf{x}_k = \mathbf{x}$. The perturbation γ_{t_k} is a Gaussian noise with variance $\sigma^2_{t_k}(\mathbf{x})$ computed from ensemble members (see [Beyou et al., 2013]).

Results The approach has been validated on synthetic turbulence data and tested on real satellite oceanic data.

The first set of experiments concerns a synthetic image sequence with images of size 256×256 showing the transport of a passive scalar by a 2D turbulent flow. This sequence is, to some extent, representative of typical satellite images depicting transport processes by oceanic streams, such as sea surface temperature or sea color images. This scalar exhibits a small diffusion, and does not respect strictly a luminance conservation assumption. The 2D turbulence is also maintained by an unknown forcing, which is thus crudely modeled in our dynamical model by a zero mean Gaussian field.

Results are compared to an other data assimilation method which can be used within this framework: the weighted ensemble Kalman filter (WEnKF, [Papadakis et al., 2010]) which also relies on an ensemble Kalman filtering step, integrated within a particle filtering framework. In [Papadakis et al., 2010], the WEnKF was used to assimilate linear observations. In case of image data that is nonlinearly related to the state of the system, these linear observations consist in pseudo-observations, *i.e.* velocity fields (and associated vorticity maps) computed from a given motion estimation technique. In the experiments below, these pseudo-observations are computed from a stochastic version of the well-known Lucas and Kanade motion

estimator [Corpetti and Mémin, 2012] applied on each pair of the image sequence, and are called SLK.

The results are first compared in terms of global RMSE between the ground truth vorticity and the estimated vorticity at each time step, and similarly for the motion fields. The WEnKF and WETKF results have been obtained with $N = 700$ particles. As may be observed on Figure 1-(a), the improvement obtained with the WEnKF filtering technique over SLK measurements is minor, and even deteriorates the results in terms of velocity fields reconstruction. The proposed WETKF technique, directly based on image luminance observations, leads to much better results for the estimation of vorticity and velocity fields.

In addition to global errors comparisons, the analysis of spectra plotted on Figure 1-(b) allows to observe more precisely the accuracy of the different techniques at different scales. As a matter of fact the RMSE constitutes only a performance measure at large scales. Note that the scale of Figure 1-(b) is given in units of the inverse of the image size. For instance, the scale 10 corresponds to 25 pixels, the scale 10^2 corresponds to 2,5 pixels. It is interesting to note that all methods give relatively coherent results only from the large scales up to the beginning of the inertial range. On the other hand, the result obtained with the WETKF assimilation scheme is closer to the ground truth over the whole scale range (from the largest scales up to the small dissipative scales). This comes from the fact that this technique can take benefit of all available information in the image data, while pseudo-observations given by a local motion estimator will not be able to improve the estimation at all scales. Filters based on pseudo-observations are unable to correct the loss of energy caused by the smoothing operator used in the external estimation procedure.

For a qualitative visual comparison, estimated vorticity maps are plotted on Figure 2 at a given time instant. The scalar image observation is first presented, together with the ground truth vorticity on Figure 2(b). Figure 2(c) shows the vorticity estimated with the local SLK technique. The result obtained with the WEnKF assimilation scheme based on these SLK observations is presented on Figure 2(d), while Figure 2(e) shows the result obtained with the proposed WETKF technique, assimilating image data directly. As can be seen on Figure 2(c), the vorticity estimated by the local motion estimation technique is far from the ground truth. As a consequence, the WEnKF assimilation based on these measurements only brings a small improvement since these observations do not carry enough information. The solution lacks clearly of energy compared to the true vorticity. The direct assimilation of image data through the WETKF scheme leads to a better estimation of vorticity structures, and in particular of small scales structures as discussed

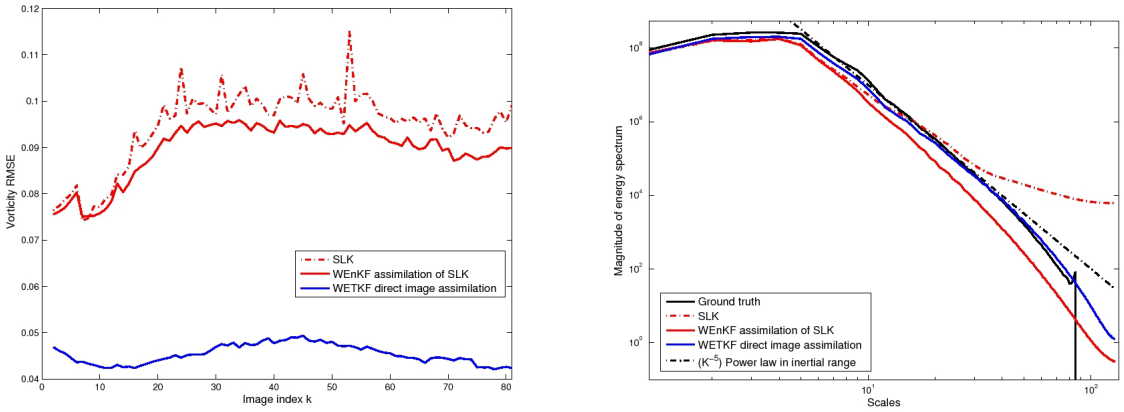

(a) (b)

Figure 1: Synthetic 2D turbulent flow. (a) RMSE between mean estimate of vorticity and ground truth; (b) Energy spectra.

previously with the comparison of spectra.

The second set of results concerns the application of the proposed WETKF technique on satellite images of Sea Surface Temperature (SST), with large areas of missing data due to the cloud cover and presence of coastal regions. The sequence consists of 48 images of size 256×256. These images come from the MetOp satellite (AVHRR radiometer) and have been provided by CERSAT laboratory of IFREMER. The images have a spatial resolution of 0.1 degree (10 km) and a temporal latency of 24 hours. The sequence is centered on an area of the Pacific ocean off the Panama isthmus and shot during an El Niño-Southern oscillation. Representative results at different time instants of the sequence are shown in Figure 3. The first column of Figure 3 shows the estimated velocity fields at times $k = 1, 10, 24$ and $k = 39$, superimposed on the corresponding SST images. The second column shows the estimated vorticity maps and velocity fields. The initialization for image 1 is based on the estimation provided by the local motion estimation approach (SLK). We see that this initialization provides only a rough large scale motion field. This estimate is refined afterward by the filtering process. We can note that the motion fields estimated along the sequence stick quite well to the big image structures observed on the SST images. The sequence of motion fields does not seem to be perturbed by the big missing data regions observed intermittently. Finally, we can note that the result obtained shows well an increase of the turbulent agitation that can be readily observed on the SST image sequence.

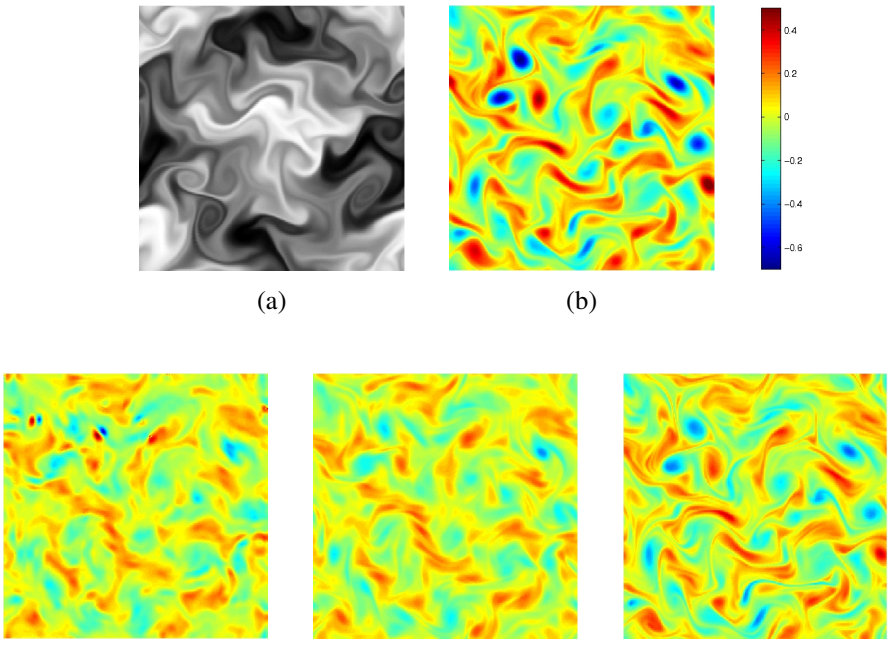

Figure 2: Synthetic 2D turbulent flow. (a) Example of scalar image of the sequence at given time k; (b) Ground truth vorticity at time k; (c) SLK vorticity estimate; (d) Mean estimate of vorticity with WEnKF assimilation of SLK observation; (e) Mean estimate of vorticity with WETKF direct assimilation of image data.

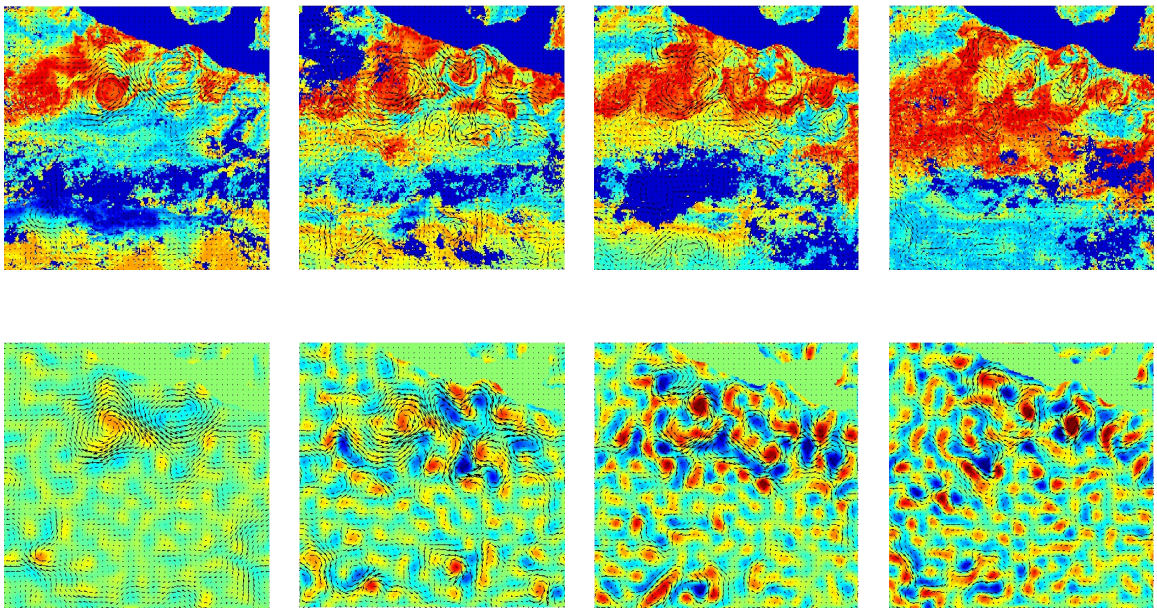

Figure 3: Real satellite sequence of SST (sea surface temperature) images. Dark blue regions indicate missing data due to the cloud cover or land regions. First row: SST images at different days $k = 1, 10, 24, 39$ and estimated velocity fields with the WETKF assimilation of image data; Second row: Mean estimated vorticity with WETKF and associated velocity fields.

However, one can identify many small scale vortices in the estimation results that may not be physically relevant. A better characterization of the dynamical noise could help correcting these artefacts.

To conclude this section, let us note that the computational cost of the hybrid WEnKF of WETKF method is the same as the one of EnKF or ETKF, since only a weighting step is added.

2.4 Conditional simulation for image data assimilation

The image data (given by satellites for instance) offer a high spatial resolution but a low temporal resolution, so that the time step between observations can be long in the assimilation scheme. This may cause discontinuities in the assimilation result, since the filtering relies on the dynamical model only between observations.

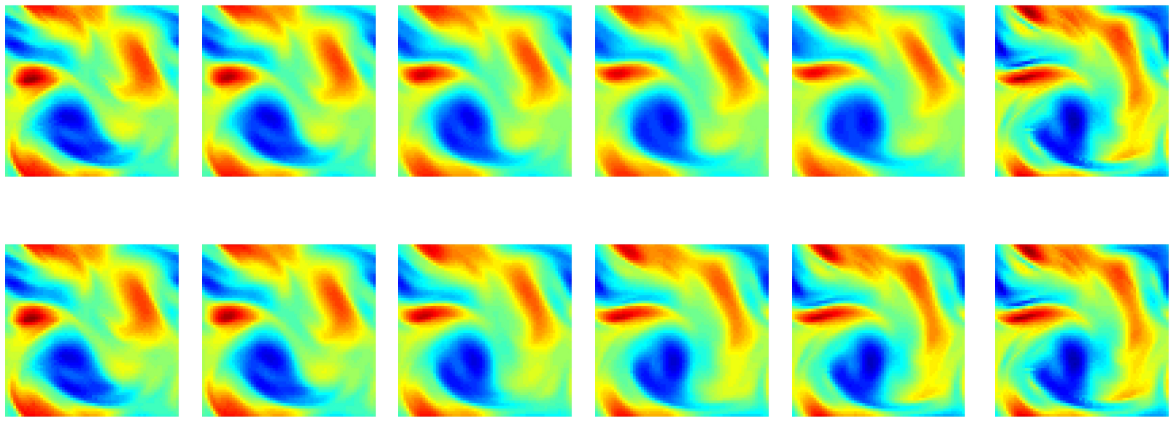

Figure 4: First row: Illustration of the discontinuity in the particle filtering result between two observation times t_k and t_{k+1}; Second row: Result after the smoothing procedure based on conditional simulation proposed in [Cuzol and Mémin, 2013].

In order to reduce such discontinuities and avoid the estimation of state trajectories that are not physically consistent, one can use a Monte Carlo sequential smoothing technique based on conditional simulation of diffusions [Delyon and Hu, 2006]. This technique, proposed in [Cuzol and Mémin, 2013], relies on the filtering result and allows the sampling of continuous smoothed trajectories between observation times. The method can be applied to non linear and multidimensional models. An example is given in Figure 4, related to the estimation of a turbulent flow from images. The experimental setup is similar to the one presented in Section 2.3. The filtering and smoothing results are given as illustration between two given observation times t_k and t_{k+1}. The temporal discontinuity in the filtering result can be seen on the first row, while the second row shows the result after smoothing.

This promising technique can be extended to build alternative data assimilation techniques for data that are observed without noise (or very small noise). In that case, the assimilation problem can be formulated as the conditional simulation of a partially observed model, where the state (the vorticity for instance) is gradually corrected toward the observations (image data). The aim is then to avoid the discontinuities between observation times and to provide smoothed trajectories in a sequential way without post-processing. This work in progress is based

on the theoretical results presented in [Marchand, 2012, Marchand, 2013].

3 Conclusion and perspectives

In this paper we have shown how a Kalman ensemble technique can be embedded within a particle filter. The resulting technique compared to ensemble filtering techniques allows robustifying the filtering and provides improved results. It opens also a way to assimilate different observations attached either to the particle filtering stage or to the sampling step, encoded through the ensemble Kalman filter mechanism. Such an ability has not been yet experimentally assessed and we plan to explore it in a near future. The hybrid filters show standard limitations associated to filtering issues where a continuous dynamics is coupled with a discrete sequence of observations. In that case an implausible trajectory is generated by a violent correction at observation times. We have described briefly how to correct a posteriori this deficiency with a fixed lag smoothing. This conditional simulation approach can be extended to built a data assimilation method associated to the ill-posed case of low observation noise. We are currently exploring this promising technique.

References

[Avenel et al., 2013] Avenel, C., Mémin, E., and Pérez, P. (2013). Stochastic level set dynamics to track closed curves through image data. *Journal of Mathematical Imaging and Vision, accepted for publication*.

[Beyou et al., 2013] Beyou, S., Cuzol, A., Gorthi, S., and Mémin, E. (2013). Weighted ensemble transform kalman filter for image assimilation. *Tellus A*, 65(18803).

[Bishop et al., 2001] Bishop, C., Etherton, B., and Majumdar, S. (2001). Adaptive sampling with the ensemble transform Kalman filter. part i: Theoretical aspects. *Monthly weather review*, 129(3):420–436.

[Corpetti et al., 2009] Corpetti, T., Héas, P., Mémin, E., and Papadakis, N. (2009). Pressure image asimilation for atmospheric motion estimation. *Tellus*, 61A:160–178.

[Corpetti and Mémin, 2012] Corpetti, T. and Mémin, E. (2012). Stochastic uncertainty models for the luminance consistency assumption. *IEEE Transaction on Image Processing*, 21(2):481–493.

[Cuzol et al., 2007] Cuzol, A., Hellier, P., and Mï¿½min, E. (2007). A low dimensional fluid motion estimator. *Int. Journ. on Computer Vision*, 75(3):329–349.

[Cuzol and Memin, 2009] Cuzol, A. and Memin, E. (2009). A stochastic filtering technique for fluid flows velocity fields tracking. *IEEE Trans. Pattern Analysis and Machine Intelligence*, 31(7):1278–1293.

[Cuzol and Mémin, 2013] Cuzol, A. and Mémin, E. (2013). Monte carlo fixed-lag smoothing in state-space models. *Preprint, arXiv:1310.1267*.

[Del Moral, 2004] Del Moral, P. (2004). *Feynman-Kac Formulae Genealogical and Interacting Particle Systems with Applications*. Springer, New York; Series: Probability and Applications.

[Delyon and Hu, 2006] Delyon, B. and Hu, Y. (2006). Simulation of conditioned diffusions and applications to parameter estimation. *Stochastic Processes and Applications*, 116:1660–1675.

[Doucet et al., 2000] Doucet, A., Godsill, S., and Andrieu, C. (2000). On sequential monte carlo sampling methods for Bayesian filtering. *Statistics and Computing*, 10(3):197–208.

[Evensen, 1994] Evensen, G. (1994). Sequential data assimilation with a non linear quasi-geostrophic model using Monte Carlo methods to forecast error statistics. *J. Geophys. Res.*, 99 (C5)(10):143–162.

[Evensen, 2003] Evensen, G. (2003). The ensemble Kalman filter, theoretical formulation and practical implementation. *Ocean Dynamics*, 53(4):343–367.

[Franzke and Majda, 2005] Franzke, C. and Majda, A. (2005). Low-order stochastic mode reduction for a prototype atmospheric gcm. *J. Atmos. Sci.*, 63:457–479.

[Gordon et al., 1993] Gordon, N., Salmond, D., and Smith, A. (1993). Novel approach to non-linear/non-gaussian bayesian state estimation. *IEEE Processing-F*, 140(2).

[Houtekamer and Mitchell, 1998] Houtekamer, P. L. and Mitchell, H. (1998). Data assimilation using an ensemble Kalman filter technique. *Monthly Weather Review*, 126(3):796–811.

[Kalman, 1960] Kalman, R. (1960). A new approach to linear filtering and prediction problems. *Transactions of the ASME - Journal of Basic Engineering*, 82:35–45.

[Le Gland et al., 2011] Le Gland, F., Monbet, V., and Tran, V. D. (2011). Large sample asymptotics for the ensemble Kalman filter. In Crisan, D. and Rozovskii, B., editors, *Handbook on Nonlinear Filtering*, pages 598–631. Oxford University Press.

[Majda et al., 1999] Majda, A., Timofeyev, I., and Eijnden, E. V. (1999). Models for stochastic climate prediction. *PNAS*.

[Marchand, 2012] Marchand, J. (2012). *Conditionnement de processus markoviens*. PhD thesis, IRMAR, Université de Rennes I.

[Marchand, 2013] Marchand, J. L. (2013). Conditioning diffusions with respect to partial observations. *Preprint, arXiv:1105.1608*.

[Mémin, 2013] Mémin, E. (2013). Fluid flow dynamics under location uncertainty. *Geophysical & Astrophysical Fluid Dynamics*. accepted for publication.

[Ott et al., 2004] Ott, E., Hunt, B., Szunyogh, I., Zimin, A., E.J. Kostelich, M. C., Kalnay, E., Patil, D., and Yorke, J. A. (2004). A local ensemble Kalman filter for atmospheric data assimilation. *Tellus*, 56A:415–428.

[Papadakis et al., 2010] Papadakis, N., Mémin, E., Cuzol, A., and Gengembre, N. (2010). Data assimilation with the weighted ensemble Kalman filter. *Tellus Series A: Dynamic Meteorology and Oceanography*, 62(5):673–697.

[Snyder et al., 2008] Snyder, C., Bengtsson, T., Bickel, P., and Anderson, J. (2008). Obstacles to high-dimensional particle filtering. *Monthly Weather Review*.

[Titaud et al., 2010] Titaud, O., Vidard, A., Souopgui, I., and Dimet, F.-X. L. (2010). Assimilation of image sequences in numerical models. *Tellus A*, 62(1):30–47.

[Van Leeuwen, 2010] Van Leeuwen, P. J. (2010). Nonlinear data assimilation in geosciences: an extremely efficient particle filter. *Quarterly Journal of the Royal Meteorological Society*, 136(653):1991–1999.